On Time-series Topological Data Analysis: New Data and Opportunities

Lee M. Seversky
Air Force Research Laboratory
Lee.Seversky@us.af.mil

Shelby Davis
Black River Systems
Davis@brsc.com

Matthew Berger
Air Force Research Laboratory
Matthew.Berger.1@us.af.mil

Abstract

This work introduces a new dataset and framework for the exploration of topological data analysis (TDA) techniques applied to time-series data. We examine the end-to-end TDA processing pipeline for persistent homology applied to time-delay embeddings of time series – embeddings that capture the underlying system dynamics from which time series data is acquired. In particular, we consider stability with respect to time series length, the approximation accuracy of sparse filtration methods, and the discriminating ability of persistence diagrams as a feature for learning. We explore these properties across a wide range of time-series datasets spanning multiple domains for single source multi-segment signals as well as multi-source single segment signals. Our analysis and dataset captures the entire TDA processing pipeline and includes time-delay embeddings, persistence diagrams, topological distance measures, as well as kernels for similarity learning and classification tasks for a broad set of time-series data sources. We outline the TDA framework and rationale behind the dataset and provide insights into the role of TDA for time-series analysis as well as opportunities for new work.

1. Introduction

Topological data analysis (TDA) has shown to be a powerful tool for analyzing complex data sets. Techniques such as persistent homology [11] have led to new insights and methods for exploring the topological properties and *shape* of data. TDA techniques have been applied to diverse problem sets including 3D shape matching [4, 26], recurrent system modeling [30], and periodicity detection [25]. Of recent interest is the exploration and application of TDA to time-delay embeddings of time series for the modeling and classification of dynamical systems and time-varying events [33, 24, 34].

Time-delay embeddings have primarily been considered in the context of analyzing dynamical systems [31], where a time-delay embedding of time-series data can be used to recover the underlying dynamics of a system. As a result, the time-delay embedding model has been used by a number of techniques including chaotic attractors [2] and more recently considered jointly with TDA, for example, in analyzing human speech [3] and classification [24, 12]. While TDA techniques show promise as a powerful descriptor for modeling and understanding time-series, there currently does not exist a comprehensive study characterizing these techniques in the context of broader types of time-series sources that are currently being considered by the larger research community.

This work is motivated by two recent and growing trends in TDA. First, with the development of more computationally efficient TDA techniques [29, 9, 16], it is now possible to consider larger and more realistic datasets. For example, the recently introduced sparse filtration technique [29] enables linear-size approximations of the Vietoris-Rips filtration, which is a core component for many TDA tasks, and enables the efficient construction of persistence diagrams. Similarly, the recent *geometry-aware* technique [16] for computing Wasserstein and Bottleneck distances on persistence diagrams provides a computationally efficient means for measuring similarity across persistence diagrams. With these advancements come new opportunities in TDA and time-series applications, such as change point detection [15], motif finding [18], and classification [3].

Second, there has been a growing trend in exploring how topological information can be used to form *geometry* and *topology* enriched representations for machine learning [22, 21]. While techniques for building topological features have been developed, it has been only recent that topology has been considered in the context of the large class of kernel-based learning techniques. In [26], a multi-scale kernel for persistence diagrams is introduced that defines a persistence scale space kernel, providing the connection between persistence diagrams and widely-used kernel based techniques, such as SVM and PCA.

With these new opportunities in TDA come new challenges. To date, there does not exist a comprehensive topological dataset targeted to both practitioners and researchers alike for exploring topological properties and performance of TDA techniques against well-studied time-varying data

sets. To address this gap, this work introduces a new time-series topology dataset, *TS-TOP* and a framework for capturing the end-to-end TDA processing and data pipeline. We discuss the processing pipeline and new dataset and explore the sensitivity and applicability of TDA methods for characterizing complex time-varying events and dynamics.

The goal of the dataset and framework is to identify new opportunities for applying TDA to new domains and make accessible datasets and advanced topological techniques to researchers outside the topology community. We hope that this work can help to further development of efficient computational tools and new TDA based learning applications.

2. Time-series TDA Processing Pipeline

In this section, we introduce the main components of our time-series processing framework that was used to create the TS-TOP dataset. Different from existing publicly available computational frameworks targeted for general TDA [32, 20, 19], our framework explicitly considers TDA in the context of time-series analysis, where the focus is on exploring topological properties with respect to different delay-embeddings, approximations, and time-series learning tasks. Our time-series processing pipeline is shown in Figure 1.

Time-delay Embedding: Following [23, 31] for general time-series data and built upon by [25] to explore topological properties of 1-dimensional time-varying signals, we construct a time-delay embedding of the input signal. The embedded signal is then partitioned into segments of a specified length.

Formally, given a 1-dimensional signal f of length n, the time-delay embedding of f is the set of points $X = (x_t, x_{t+1}, \ldots, x_{t+(n-m)})$, where $x_t = (f_t, f_{t+1}, \ldots, f_{t+m})$ and $x_t \in \mathbb{R}^{m-1}$. While it is possible to examine the topology using all of X, for time-series it is of interest to examine the embedded points as a function of time. Therefore, for single-source continuous signals, we partition X into a set of segments $\{S\}_j$, such that $s_j = (x_j, x_{(j+1)}, \ldots, x_{(j+k)})$, where k is the segment length and j is the segment start. For multi-source signals, we represent each signal source as one segment, such that the point cloud X comprises a single segment. Additional details of the dataset types can be found in Section 3.

Persistence Diagrams: Given the segments, we wish to explore the topology of each segment through the analysis of the embedded point cloud and its persistence diagram. Persistence diagrams [10] provide a concise description of the topological changes over all scales of the data. This multiple scale viewpoint of the data can be realized via persistent homology [10] through a filtration on the data which captures the growth, birth, and death of different topological features across dimensions (e.g. components, tunnels, voids). From this filtration, the birth and death of a k-dimensional component can be described by a point (a, b) in the persistence diagram of dimension k, where a, b is the birth and death times respectively. A key challenge associated with computing persistence is its dependence on the filtration size, which grows as $O(n^{k+1})$ for simplices up to dimension k. We use the recent sparse Vietoris-Rips filtration [29] to produce a linear-size filtration, which is then used in the computation of the persistence diagram via the standard pairing algorithm [10].

The persistence diagram is comprised of the set of all k-dimensional birth-death pairs forming a multiset of points in $\mathbb{R}^2$. These pairings capture the topology of the space across all scales such that a significant topological feature *persists* as a function of time [10]. Specifically, we are interested in exploring the 1-dimensional persistence diagrams, which provides a concise description of topological 1-dimensional cycles that may exist in the data. This is particularly informative, as such cycles can provide insights into periodic and repetitive patterns often found in time-series data and can serve as important discriminating descriptors [25]. Therefore, we focus our efforts on computing and analyzing 1-dimensional persistence diagrams for the characterization of periodic and repetitive patterns.

Distance Measures: Given persistence diagrams it is only natural to want to compare diagrams with respect to topological similarity. A distance metric for persistence diagrams provides a means for relating the topology of data and more generally the datasets in terms of topological similarity and has received much attention [1, 14]. In general persistence diagrams are stable, where small changes in the data results in small changes in the diagram [7]. Two common distance metrics are the Wasserstein and Bottleneck distances. Wasserstein distance is defined as the sum of the q-th powers of the distances between points across all matchings between persistence diagrams. A specialization of the Wasserstein distance is the bottleneck distance, which is the Wasserstein distance in the limit as q goes to infinity, and is the largest distance between two points in the best matching [10]. In the case of the bottleneck distance it is stable with respect to perturbations [7]. We use these distance measures to compute all-segment pairwise distances across all time-series datasets utilizing recent efficient techniques introduced in [16].

Topological Kernels: A growing area of interest is the use of topological information for machine learning tasks. Prior approaches focused on featured-based descriptors built directly from persistence diagrams. For example, in [22] the persistence diagrams are rasterized as images and an image-based feature is then derived and used to build a standard image-based kernel to train an SVM classifier. Such approaches impose arbitrary representations on top of the persistence diagram in order to utilize traditional learning techniques with topology. Alternatively, [17] considers

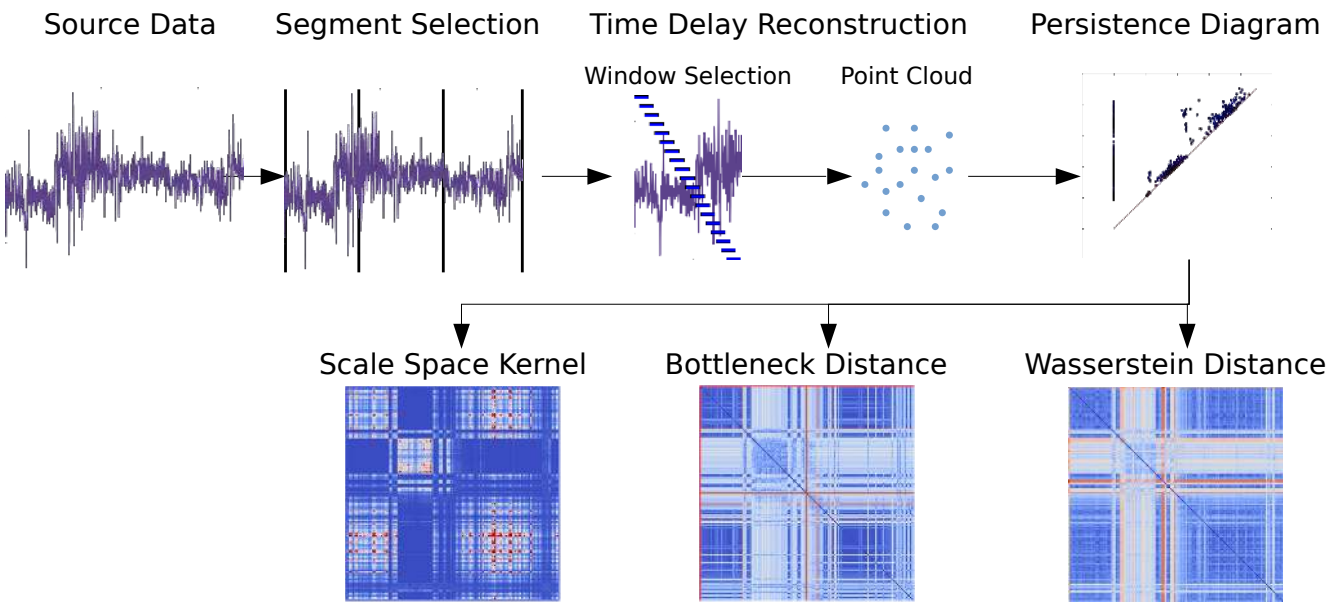

Figure 1: TDA processing pipeline for time-series analysis: Our framework enables end-to-end configuration and inspection of each processing stage beginning with partitioning the input signal into segments, time-delay embedding, and computation of persistence diagrams, as well as multiple distance measures and kernels. The pipeline is fully configurable and automated.

the Wasserstein and Bottleneck distance measures for the task of recognition by formulating the problem as a nearest neighbor finding task. While using similarity for recognition is well motivated, it is also desirable to consider topology with a larger class of machine learning techniques.

The recent work of [26] provides a bridge between topology and the class of popular kernel-based learning methods, such as kernel support vector machines (SVM) and kernel PCA. These techniques are advantageous for learning as they do not require an explicit feature representation and are generally efficient to compute. In [26], a new multi-scale kernel is derived based on heat diffusion of points in the persistence diagram, and is shown to be stable with respect to the 1-Wasserstein distance. Using this approach, learning tasks such as classification can be performed by constructing kernels directly from the persistence diagrams.

3. A Time-series Topology Dataset (TS-TOP)

Datasets provide a critical tool for research and exploration. This is especially important for TDA, where there is much interest in seeking out new applications that build upon the strong theoretical foundations developed by the topology community. However, to fully explore the applicability of topological techniques for both researchers and practitioners, a comprehensive dataset is advantageous.

We address this gap by developing a topology time-series dataset that captures, stores, and explores the end-to-end TDA pipeline for a diverse set of time-series datasets. Specifically, the work considers two broad types of time-series sources: (1) single-source continuous signals that can be decomposed into a series of temporal segments and (2) multi-source single segment signals, where there are multiple signal sources and each source signal is its own segment. For both data types we consider a diverse collection of time-series data that have been annotated and used by the research community for time-series analysis. A short description of each dataset is provided below:

Single-source Continuous Signals:

- **Activity [5]**: Three-dimensional accelerometer measurements capturing movements for 15 human participants and 7 daily activities.
- **Walking [5]**: Three-dimensional accelerometer measurements of 22 people walking along predefined and free-form paths.
- **MOCAP [8]**: Motion capture data capturing multiple types of human motion.
- **Kitchen [8]**: Motion capture data capturing multiple prescribed kitchen tasks.
- **EEG [28]**: EEG sensor data capturing eye state.
- **PAMAP [27]**: Physical Activity Monitoring for Aging People: human motion measurements for 19 different activity types.
- **Bird Sounds [13]**: Audio recordings of different bird species with multiple recordings per species type.

Multi-source Signals:

- **UCR [6]**: 47 time-series datasets broadly categorized by type: Image, Motion, Sensor, & Simulation. The segment size is set to the signal length and the window size is varied. The same features, distances, and kernels are computed, as outlined in Table 1.

Dataset	Records	Dim	Classes	Seg. Size	Win. Size	Features	Distances	Kernel
Activity [5]	1,926,896	3	7	1000, 2000	50,100,150	$PD^{0,1}$	W,B	SSK, RBF
Walking [5]	149,322	3	22	200	15	$PD^{0,1}$	W,B	SSK, RBF
Mocap [8]	225,551*	62	2*	150	15	$PD^{0,1}$, CI	W,B	SSK
Kitchen [8]	17,726,895	9	5	1000	120	$PD^{0,1}$	W,B	SSK, RBF
EEG Eye [28]	14,980	16	2	300	20	$PD^{0,1}$	W,B	SSK, RBF
PAMAP [27]	2,872,533	52	19	1000	20,30,40,50	$PD^{0,1}$	W,B	SSK, RBF
Bird Sounds [13]	24,050,377	1	16	800	15,30,45	$PD^{0,1}$	W,B	SSK, RBF

Table 1: Single-source continuous time-series datasets, where feature types are PD^x for the x-dimensional persistence diagram and CI is the chaotic invariant feature [2]. *W* and *B* are the Wasserstein and Bottleneck distances, respectively. *SSK* is the scale-space kernel [26], and RBF is the Radial Basis kernel. Note only the *Run* and *Walk* labels are included for CMU Mocap.

Additional statistics about the single-source datasets can be found in Table 1 and the list of multi-source datasets from the UCR collection are listed in Figure 5.

4. Analysis of TDA for Time Series

A main result of the time-series topology dataset and framework is that it enables the exploration of a broad set of time-series data sources with respect to their topological properties, as well as enhances understanding of the applicability and limitations of current TDA techniques. In this section, we apply our processing pipeline to the datasets listed in Section 3 and discuss initial findings.

For each dataset, we partition the input signals into a series of segments, compute delay coordinate embeddings, and generate persistence diagrams. Each stage is fully tunable, where segment size, segment overlap, and window size (embedding dimensionality) can be controlled. Further, we compute the linear-sized approximate Rips filtration [29], with the ability to compute the full Rips filtration, when generating the persistence diagrams, allowing us to explore how well topological features are preserved and discover any application sensitivities. Finally, to explore the discriminating and learning potential of the topological information, we compute both Wasserstein and Bottleneck distances between all segment pairs and configurations, as well as the scale-space persistence kernel [26].

The full provenance of all intermediate representations and outputs for all parameter configurations are stored for each dataset. For example, for the Activity dataset there are 11,556 pre-computed segments generated across 3 dimensions and 2 segment sizes of 1000 and 2000 respectively. For each of the segments computed from the Activity dataset, we consider three window sizes (embedding dimensions) 50,100,150 yielding 34,668 point clouds for which both 0 and 1 dimensional persistence diagrams are computed. Finally, both Wasserstein and Bottleneck distances for all segment pairs for a given segment and window size are computed. Similarly, we construct the scale-space kernel. This process is repeated for each time-series dataset.

We believe this comprehensive approach to the collection of topological data to be valuable, as it enables researchers from outside the topology community to explore the space of topological information across datasets without necessarily requiring expert knowledge of the topological approaches or the investment in the time and computational resources needed to generate the data. In addition, our framework can be extended to include new datasets as well as new performance comparisons and evaluations.

The following sections highlight initial insights that were gained while examining the topological properties of the various datasets. The purpose of this discussion is to provide general findings and comparisons, it is not to provide a comprehensive survey or detailed comparison of TDA techniques against the current state-of-the-art in time-series analysis. However, we anticipate that this dataset can be used as a tool to help enable such endeavors in the future.

4.1. Approximation Sensitivity

As previously discussed, we use the linear-size sparse Vietoris Rips filtration of [29] for the computation of persistence. An attractive property of the filtration is its provable guarantees in approximating the persistence diagram with respect to the full filtration. However, the approach makes strong assumptions on the doubling dimension of the metric space formed by the point cloud. If this quantity happens to be large for a given point cloud, then the filtration size necessary to produce a target approximation can become huge.

For time-delay embeddings, we wish to see if their point distributions adhere to the metric assumptions made in [29]. Specifically, we explore the impact of the approximation as it applies to differences in the persistence diagrams between the full rips filtration and approximate version. To this end, we compare the approximation accuracy by bounding the maximum number of simplices as a function of the number of points in the delay embedding for each segment. Let k be the segment size and w be the window size, then the number of embedded points is $(k - w)$. The maximum number of simplices can be bounded by the total number of points such that the maximum simplices is $(k - w)^{d+1}$ for simplices up to dimension d [29]. This bound is used to evaluate the trade

offs between approximation accuracy and performance.

We highlight these trade offs for the Activity dataset in Figure 2. We show the Bottleneck and Wasserstein distances between the persistence diagram constructed from the Rips filtration and the approximate filtration. For each segment, we set the maximum simplices to $\alpha(k-w)^2$ and study the approximation for different values of α. The sparse filtrations are parameterized based on the maximum number of simplices allowed in the filtration – in turn this sets the approximation accuracy of the persistence diagram.

We make several observations from our results for motion-based time-series. We find that the linear-size claims of [29] require very large constants – proportional to the number of points – to obtain persistence diagrams of reasonable accuracy. This is indicative of the complexity of the time-delay embeddings, producing point clouds whose doubling dimensions are likely very large. On the positive side, we observe that the bottleneck distance tends to grow sublinearly as a function of the segment size, for sufficiently large values of α. This implies that we can afford a smaller constant α as the length of the time series increases, demonstrating the potential scalability of sparse filtrations when applied to long segments.

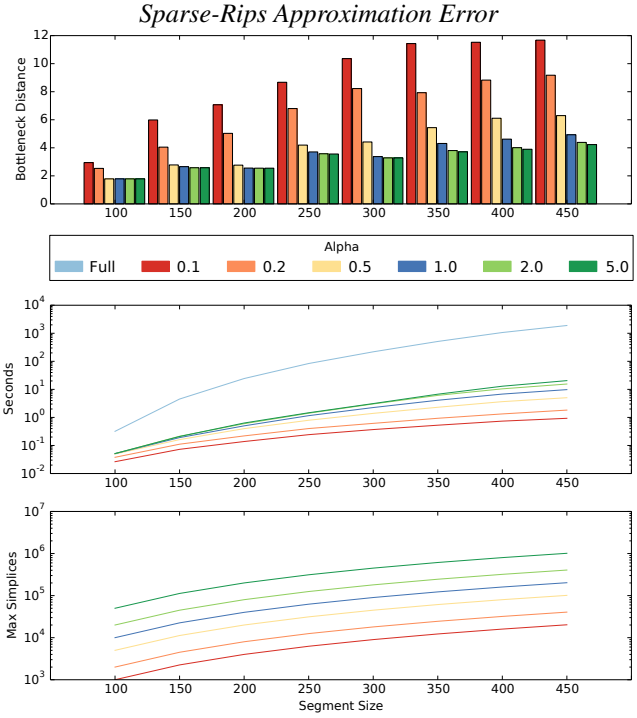

Figure 2: Approximation error in terms of distance of approximate sparse-filtration from baseline persistence diagram utilizing exact Rips filtration for increasing segment sizes and maximum simplices for the Activity dataset.

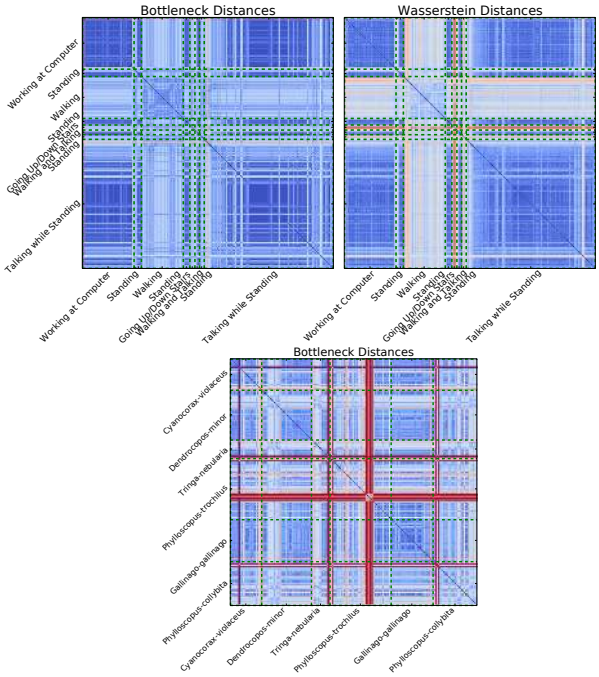

Figure 3: Top: Inter/Intra class Bottleneck and Wasserstein distances for all pairs persistence diagrams from the Activity dataset. Bottom: Bottleneck distances for Bird dataset.

4.2. Distance Measures

The Wasserstein and Bottleneck distances provide a means for comparing the topological similarity between persistence diagrams. To evaluate this similarity space with respect to different class types, we compute the distance for all pairs of persistence diagrams and classes. Figure 3 shows the distance matrices for the Activity dataset, where the segments are grouped by class label. For in class segments the distances between persistence diagrams should be close to zero, while across classes the distances should be larger. We observe that the differences in topology tends to be uniform, i.e. *Working at Computer*, while for other classes such as *Walking*, the distances between diagrams is more varied indicating larger variability in the topology of segments within the class. Likewise, classes such as *Going Up/Down Stairs* are highly discriminating as indicated by the large distances to all other classes. However, for other datasets such as the Bird dataset, the distances are not as discriminating having high variability within all classes, making distance alone insufficient for discriminating between class types as shown in Figure 3 bottom.

4.3. Classification

This section explores classification of time-series events and highlights results for both single-source continuous and multi-source dataset types.

Single-Source Continuous Signals: We investigate the classification performance across time-series data sources using the scale-space topological kernel [26] and kernel-SVM classifier. We consider the RBF kernel as our general time-series classification baseline and additionally compare with the chaotic invariant feature [2]. The chaotic invariant feature is specifically tailored to concisely modeling the dynamics described by time-series. For example it has been used in computer vision applications to describe the time-varying dynamics of trajectories, pixel intensities, and flow vectors.

In Figure 4, we compare the classification accuracy of the chaotic invariant feature and scale-space kernel across sensors and dimensions for the MOCAP dataset. First we explore how the automatic time-delay and window estimation technique outlined in [2] behaves with respect to setting the per segment delay and dimension across sensors and dimensions. Figure 4a shows the min, max, and average delay and dimension selected using the estimation technique. As shown, the parameters vary significantly as a function of both sensor source and dimension.

Next, we examine classification performance and show results for the MOCAP dataset in Figure 4b. For this experiment, we fix the segment size to 150 and consider both a fixed window of 15 as well as allow the window to vary using the automatic estimation technique of [2]. For training, the segments are divided into 100 train/test splits and cross-validation is performed to set hyperparameters for both the scale-space kernel and SVM model. For each sensor (head, lfemur, rhumerus) and dimension (0,1,2), we construct a scale-space kernel and train individual classifiers. We also average all of the kernels and similarly train a classifier using the averaged kernel. We show the classification accuracy across all kernels, where the averaged kernel achieves higher accuracy than the chaotic invariant feature indicating that the scale-space kernel can be a strong discriminator for such trajectory-based data sources. Further we show that the auto-selected per segment window size does not perform as well for classification as the fixed window size for this case, indicating that there may be key topological information that is not being captured by the smaller window sizes.

Multi-source Signals: We next explore the classification performance with respect to the UCR datasets. We characterize the discriminating ability of the scale-space kernel with respect to different window sizes and category types. The goal is to gain an increased understanding on what types of time-series data can benefit from TDA. Shown in prior work, time-delay embeddings are well suited for modeling time-series of dynamical systems [31]. We explore this property and the general informativeness of topology for classification across all UCR data set types.

Figure 5 compares the relative classification accuracy.

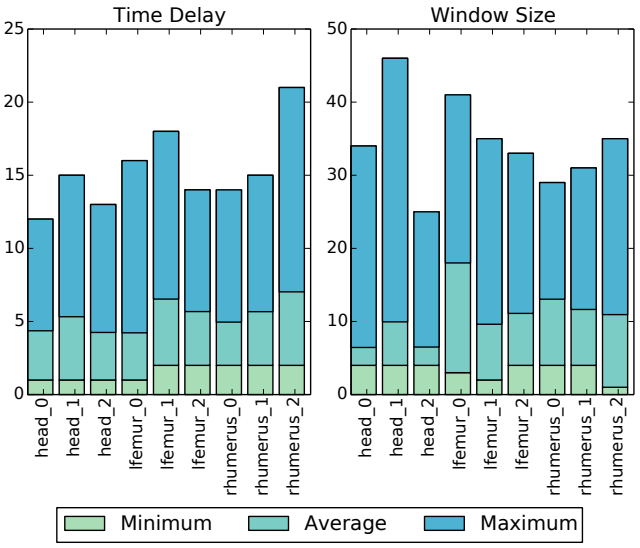

(a) Time delay and embedding size statistics for segments across sensors and dimensions using the auto estimation method from [2].

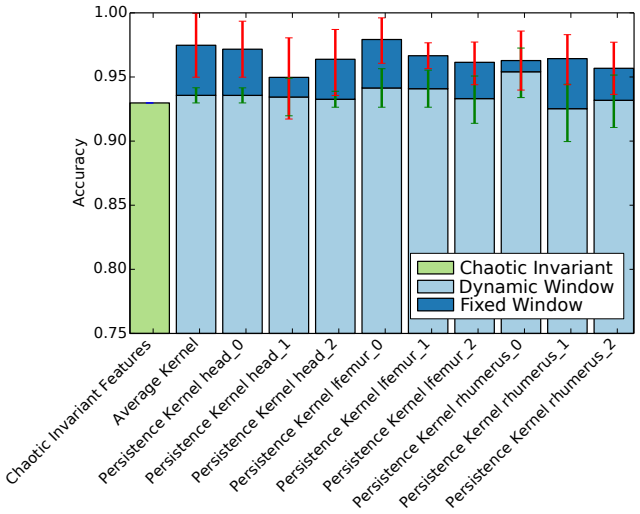

(b) Classification performance using scale-space kernel across sensors, dimensions, and averaged kernel comparing a fixed window of 15 with auto selected per segment window sizes. Chaotic Invariant feature performance provided for baseline comparison.

Figure 4: MOCAP classification comparison and analysis of time-delay and window sensitivities.

We consider window sizes of 10,20,30 and construct independent scale-space kernels for each window size and then train separate SVM classifiers. For reference, we show the performance of a SVM classifier utilizing the RBF kernel. In general the topological based kernels perform relatively well for datasets belonging to the Motion and Sensor categories and specifically for those which are physically and trajectory based, for example *SonyAIBORobotsurface* and *UWaveGestureLibraryAll*. On the other hand, non-physical based datasets such as *WordSynonyms* performs poorly as it

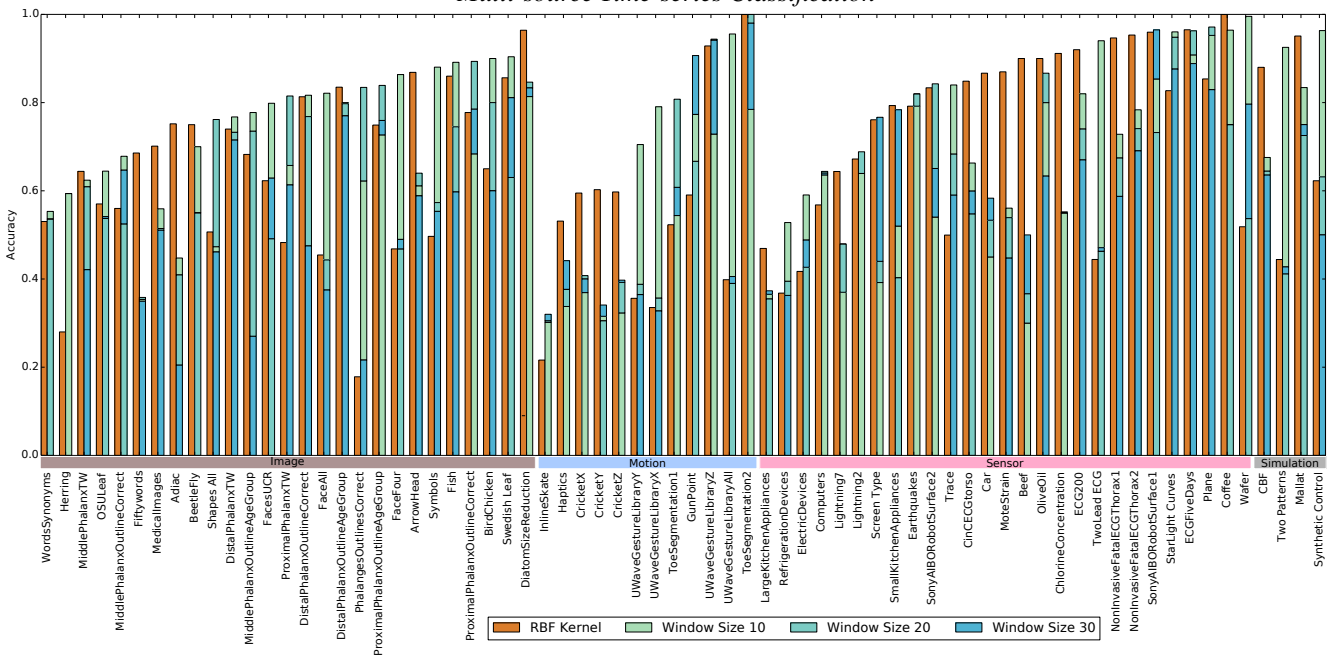

Figure 5: Classification accuracy of scale-space kernel across all UCR time-series datasets organized by data type. Results shown for window sizes of 10,20,30 with RBF Kernel performance for reference.

is unclear what discriminating topological structure should be present. In general, the results shown that TDA may be less effective for certain classes of time-series data.

To gain additional insight into the sensitivity of window size with respect to classification performance we consider the classification accuracy for different window sizes and examine the class separability of the scale-space kernel. Figure 6 shows the classification results for the UCR SonyAIBORobot dataset following the same training methodology as previously described. We also visualize the segment similarity space to highlight class separability as a function of window size by embedding the segments into 2D according to their relative scale-space similarity with all other segments. As shown, the classification accuracy is directly related to the separability of the two classes with respect to the scale-space similarity. As highlighted, selecting the correct window size requires careful consideration.

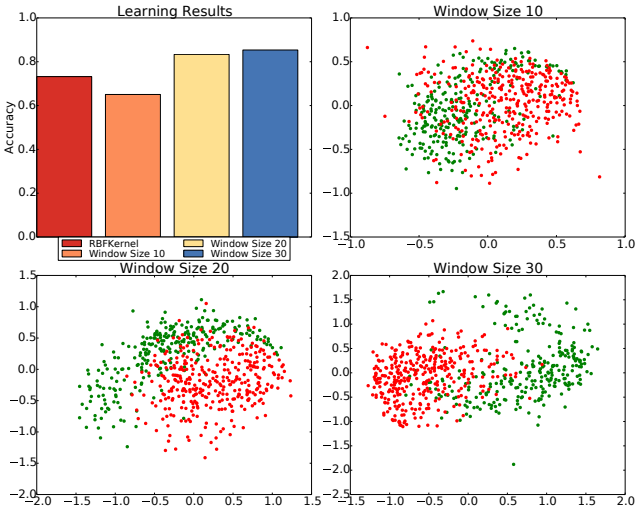

Figure 6: Delay Embedding Sensitivity: Classification results for scale-space kernel with window sizes of 10,20,30 on the UCR SonyAIBORobot dataset. Visualization depicts class separation of segments for different window sizes.

4.4. Time-varying Analysis

Finally, we examine the time-varying nature of the single-source continuous datasets, where the streaming signal describes events appearing and evolving over time. In order to better understand how the topology changes, we introduce a new tool for visualizing persistence diagrams of time-varying signals. For a given signal, we consider segments of the same class and build a probability density function over the set of persistence diagrams, where kernel density estimation (KDE) using a Gaussian kernel is used.

Figure 7 illustrates the different density functions with respect to class type for the Activity dataset. Note the strong 1-dimensional persistent features captured in the *Working at Computer* class for early birth times. On the other hand, the persistent features are more uniformly distributed for the *Standing* and *Talking while Standing* classes. Further a unique distribution at early and late birth times exists for the *Walking* class. Finally, the remaining classes exhibit lower persistent features more uniformly across all birth times, in-

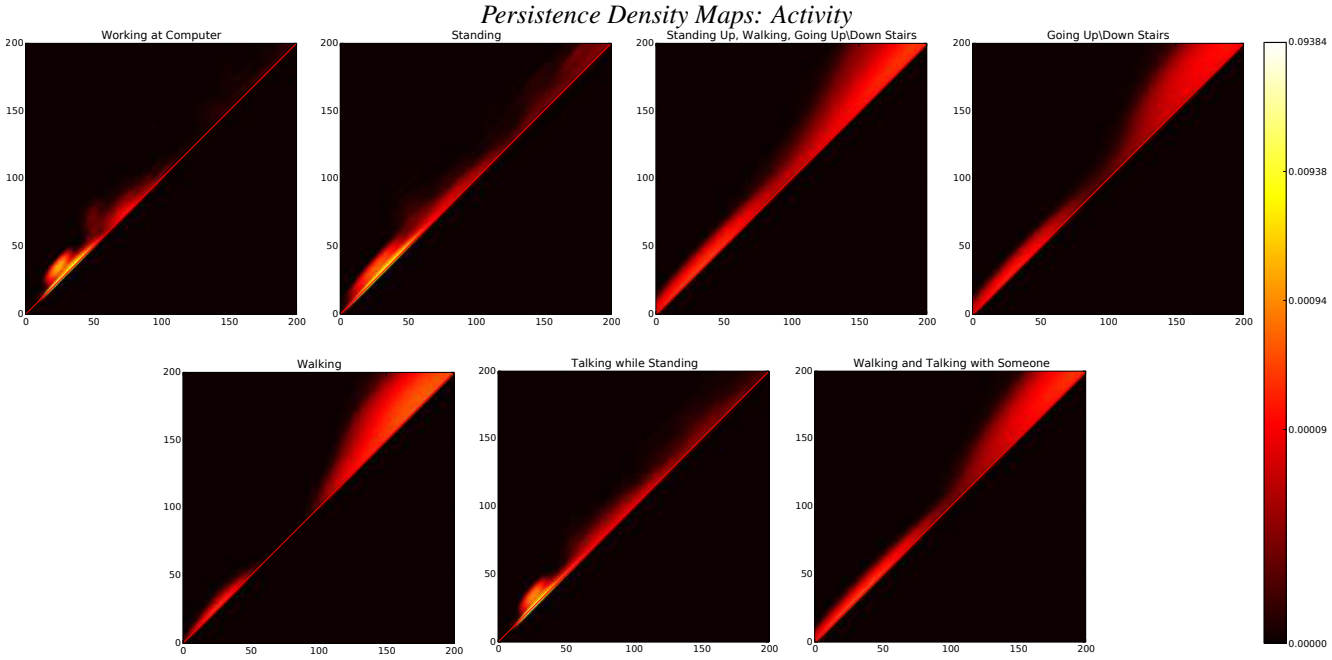

Figure 7: Density maps summarizing 1-dimensional persistence diagrams for Activity dataset for each class type.

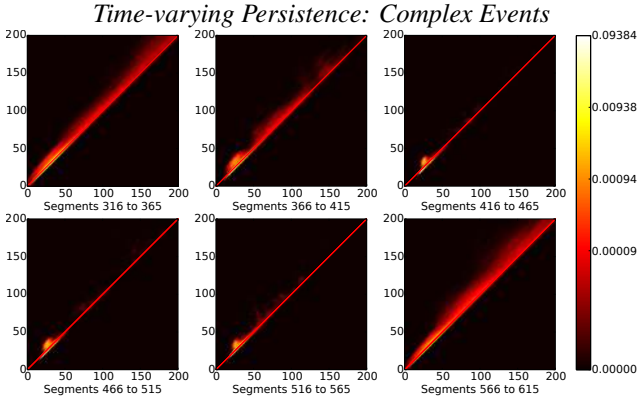

Figure 8: Fine-grained visualization of density maps for *Talking while Standing* from Activity dataset. Note evolution of persistent features for complex time-varying event.

dicating that the topological information may be less discriminating for these event types. We believe this type of visualization provides a useful and concise summarization of topological variation.

We examine one of the *less* informative classes in more detail. Specifically, consider the segments labeled *Talking while Standing*. The segments are split into three contiguous groups, where for each group, the density maps are computed. See Figure 8. With this finer-detailed summarization new interesting topological features are revealed. Specifically, we observe that for the *Talking while Standing* activity, the topology is evolving over time, taking on very different structure, where initially there are strong high persistent features with early birth times and to a lesser degree a few significant features with late birth times. However, as the action progresses the late birth time features disappear and once again reappear. This indicates that there is important information regarding the time-varying nature of the signal that is captured through topology, which is not necessarily captured by an individual analysis of the persistence diagrams. We believe this is an interesting area for future work.

5. Conclusions

This paper introduces a new time-series topology dataset, *TS-TOP* for exploring the topology of time-delay embeddings. We examine the topological properties of well-known time-series datasets and introduce a computational framework for enabling the processing, characterization, and analysis of time-series data. The main goal of the dataset and associated computing framework is to expose new opportunities for applying TDA to new domains as well as increase the accessibility of relevant datasets and advanced topological techniques to researchers from both within and outside the topological community.

References

[1] A. Adcock, D. Rubin, and G. Carlsson. Classification of hepatic lesions using the matching metric. *Computer vision and image understanding*, 121:36–42, 2014. 2

[2] S. Ali, A. Basharat, and M. Shah. Chaotic invariants for human action recognition. In *Computer Vision, 2007. ICCV*

2007. IEEE 11th International Conference on, pages 1–8. IEEE, 2007. 1, 4, 6

[3] K. A. Brown and K. P. Knudson. Nonlinear statistics of human speech data. *International Journal of Bifurcation and Chaos*, 19(07):2307–2319, 2009. 1

[4] M. Carrière, S. Y. Oudot, and M. Ovsjanikov. Stable topological signatures for points on 3d shapes. In *Computer Graphics Forum*, volume 34, pages 1–12. Wiley Online Library, 2015. 1

[5] P. Casale, O. Pujol, and P. Radeva. Personalization and user verification in wearable systems using biometric walking patterns. *Personal and Ubiquitous Computing*, 16(5):563–580, 2012. 3, 4

[6] Y. Chen, E. Keogh, B. Hu, N. Begum, A. Bagnall, A. Mueen, and G. Batista. The ucr time series classification archive, July 2015. www.cs.ucr.edu/~eamonn/time_series_data/. 3

[7] D. Cohen-Steiner, H. Edelsbrunner, and J. Harer. Stability of persistence diagrams. *Discrete & Computational Geometry*, 37(1):103–120, 2007. 2

[8] F. De la Torre, J. Hodgins, A. Bargteil, X. Martin, J. Macey, A. Collado, and P. Beltran. Guide to the carnegie mellon university multimodal activity (cmu-mmac) database. *Robotics Institute*, page 135, 2008. 3, 4

[9] T. K. Dey, F. Fan, and Y. Wang. Computing topological persistence for simplicial maps. In *Proceedings of the thirtieth annual symposium on Computational geometry*, page 345. ACM, 2014. 1

[10] H. Edelsbrunner and J. Harer. *Computational topology: an introduction*. American Mathematical Soc., 2010. 2

[11] H. Edelsbrunner, D. Letscher, and A. Zomorodian. Topological persistence and simplification. *Discrete and Computational Geometry*, 28(4):511–533, 2002. 1

[12] S. Emrani, T. Gentimis, and H. Krim. Persistent homology of delay embeddings and its application to wheeze detection. *Signal Processing Letters, IEEE*, 21(4):459–463, 2014. 1

[13] H. Goëau, H. Glotin, W.-P. Vellinga, R. Planqué, A. Rauber, and A. Joly. Lifeclef bird identification task 2014. In *CLEF2014*, 2014. 3, 4

[14] C. Gu, L. Guibas, and M. Kerber. Topology-driven trajectory synthesis with an example on retinal cell motions. In *Algorithms in Bioinformatics*, pages 326–339. Springer, 2014. 2

[15] V. Guralnik and J. Srivastava. Event detection from time series data. In *Proceedings of the fifth ACM international conference on Knowledge discovery and data mining*, pages 33–42. ACM, 1999. 1

[16] M. Kerber, D. Morozov, and A. Nigmetov. Geometry helps to compare persistence diagrams. In *Proceedings of the Workshop on Algorithm Engineering and Experiments (ALENEX)*, 2016. 1, 2

[17] C. Li, M. Ovsjanikov, and F. Chazal. Persistence-based structural recognition. In *Proceedings of the IEEE Conference on Computer Vision and Pattern Recognition*, pages 1995–2002, 2014. 2

[18] J. L. E. K. S. Lonardi and P. Patel. Finding motifs in time series. In *Proc. of the 2nd Workshop on Temporal Data Mining*, pages 53–68, 2002. 1

[19] D. Morozov. Dionysus library for computing persistent homology. *Software available at http://www. mrzv. org/software/dionysus*, 2012. 2

[20] V. Nanda. Perseus: the persistent homology software. *Software available at http://www. sas. upenn. edu/˜ vnanda/perseus*, 2012. 2

[21] L. Oudre, J. Jakubowicz, P. Bianchi, and C. Simon. Classification of periodic activities using the wasserstein distance. *Biomedical Engineering, IEEE Transactions on*, 59(6):1610–1619, 2012. 1

[22] D. Pachauri, C. Hinrichs, M. K. Chung, S. C. Johnson, and V. Singh. Topology-based kernels with application to inference problems in alzheimer's disease. *Medical Imaging, IEEE Transactions on*, 30(10):1760–1770, 2011. 1, 2

[23] N. H. Packard, J. P. Crutchfield, J. D. Farmer, and R. S. Shaw. Geometry from a time series. *Physical Review Letters*, 45(9):712, 1980. 2

[24] J. A. Perea, A. Deckard, S. B. Haase, and J. Harer. Sw1pers: Sliding windows and 1-persistence scoring; discovering periodicity in gene expression time series data. *BMC bioinformatics*, 16(1):257, 2015. 1

[25] J. A. Perea and J. Harer. Sliding windows and persistence: An application of topological methods to signal analysis. *Foundations of Computational Mathematics*, 15(3):799–838, 2015. 1, 2

[26] J. Reininghaus, S. Huber, U. Bauer, and R. Kwitt. A stable multi-scale kernel for topological machine learning. In *Proceedings of the IEEE Conference on Computer Vision and Pattern Recognition*, pages 4741–4748, 2015. 1, 3, 4, 6

[27] A. Reiss and D. Stricker. Introducing a new benchmarked dataset for activity monitoring. In *Wearable Computers (ISWC), 2012 16th International Symposium on*, pages 108–109. IEEE, 2012. 3, 4

[28] O. Rosler and D. Suendermann. A first step towards eye state prediction using eeg. In *AIHLS 2013, International Conference on Applied Informatics for Health and Life Sciences*, Istanbul, Turkey, September 2013. AIHLS. 3, 4

[29] D. R. Sheehy. Linear-size approximations to the vietoris–rips filtration. *Discrete & Computational Geometry*, 49(4):778–796, 2013. 1, 2, 4, 5

[30] P. Skraba, V. de Silva, and M. Vejdemo-Johansson. Topological analysis of recurrent systems. In *NIPS 2012 Workshop on Algebraic Topology and Machine Learning, December 8th, Lake Tahoe, Nevada*, pages 1–5, 2012. 1

[31] F. Takens. *Detecting strange attractors in turbulence*. Springer, 1981. 1, 2, 6

[32] A. Tausz, M. Vejdemo-Johansson, and H. Adams. Javaplex: A research software package for persistent (co) homology. *Software available at http://code. google. com/javaplex*, 2011. 2

[33] C. M. Topaz, L. Ziegelmeier, and T. Halverson. Topological data analysis of biological aggregation models. *PloS one*, 10(5), 2015. 1

[34] V. Venkataraman, K. N. Ramamurthy, and P. Turaga. Persistent homology of attractors for action recognition. *arXiv preprint arXiv:1603.05310*, 2016. 1